

On-line Identification of Seeds in Mandarins with Magnetic Resonance Imaging

N. Hernández-Sánchez , P. Barreiro , J. Ruiz-Cabello

Physical Properties Laboratory-Advanced Technologies in Agrofood, E.T.S.I.A., Polytechnic University of Madrid, Spain, Avda. de la Complutense s/n, 28040 Madrid, Spain; e-mail of corresponding author: n.hernandez@upm.es
Instituto de Estudios Biofuncionales, Complutense University of Madrid, Madrid, Spain

Mandarins have been inspected using magnetic resonance imaging (MRI) in order to detect the presence of seeds. To enhance contrast between seeds and pulp, effective transverse relaxation time-weighted fast low angle shot images (703 ms acquisition time) were acquired. Stationary fruits were imaged and then the images were segmented to extract several features. The maximum radius of the region containing the seeds and the central axis r_{max} , and the perimeter of this region P were the most powerful features for discrimination between seedless and seed-containing fruits. Such features were the most robust since they showed the lowest noise-to-signal ratios (N/S). The proportions of correct classification were 88.9% and 86.7% for seedless and seed-containing fruits, respectively, under MRI stationary conditions. The performance under on-line conditions was evaluated by imaging the fruits while conveyed at 54 mm/s. An analysis of variance with the features extracted from the static images and the motion-corrected dynamic images showed that there were statistically indistinguishable. The proportions of correct classification were 92.5% and 79.5% for the seedless and seed-containing category, respectively, under MRI dynamic conditions. Reduction in the distance between categories for r_{max} was addressed as the main cause for the decrease in discrimination performance. The robustness of the motion correction procedure was highlighted by the low differences in the N/S ratio and the noise-to-measured range ratios between static and dynamic features.

1. Introduction

Citrus are one of the most important fruits in worldwide trade. Cultivation is spread out all over the mild climate zones, the highest production being concentrated in countries such as United States, China, Spain and Mexico. A high percentage of such production is earmarked for export and therefore fruit quality is required to be carefully assessed. Regarding the commercial strategy, inspection has to be performed on a large amount of fruit with minimum time allocation. On-line internal quality measurement in the range between 2 and 10 fruits per second is typically a key issue for inspection (Barreiro *et al.*, 2004).

One of the main concerns for citrus producers is the presence of seeds within oranges and mandarins. For consumer demand, seeds are especially undesirable in mandarin.

The absence of external evidence of seeds invokes techniques capable of performing non-destructive internal inspection. Both magnetic resonance (MR) in general and magnetic resonance imaging (MRI) in particular have demonstrated such a capability in a number of applications on fruits and vegetable quality, such as detection of bruising, internal browning, mealiness, sugar content, *etc.*, as extensively reviewed by Hills and Clark (2003) with more than 50 applications cited in the period from 1986 to 2002.

Concerning MRI detection of seeds in citrus, the acquisition of MR images where seeds are distinguishable from juice segments is the most promising procedure to be applied. Blasco *et al* (2003) demonstrated that obtaining high-quality contrast between seeds and flesh is feasible although time consuming (7s) and so only available for off-line conditions at that stage. A compromise between spatial resolution,

Notation

A_{hyp}	hypo-intense signal region, number of pixels	R_{sc}	seed and central axis region in red green blue images to region of interest ratio
A_{int}	region of interest, number of pixels	R_h	hypo-intense signal region to region of interest ratio
C	compactness of hypo-intense region, pixel^{-1}	r_{max}	maximum distance from the centre of the region of interest to P , number of pixels
M_R	measured range	T_2^*	effective transverse relaxation time, ms
N/S	noise to signal ratio		
n	number of observation		
P	perimeter of the hypo-intense signal region, number of pixels		
R_{cr}	compactness to radius ratio, pixel^{-2}		

contrast and acquisition time has to be reached in order to enhance the interest of MRI application for on-line purposes. Thus, Hernandez *et al.* (2005) acquired axial MR fast images (780 and 390 ms acquisition time, respectively) achieving a reasonable contrast for seeds within citrus under static conditions. When conveying fruits, at a rate of 54 mm/s, however, a large decrease in image quality was found when compared to the static ones. Image blurring in such study was caused by the superposition of signals from the different tissues crossing the slice being imaged during the acquisition time. Hernandez *et al.* (2005) showed an alternative slice location and a development of an algorithm for automated motion correction, on the basis of medical applications focused on correcting the effects of the patient motion (Ehman & Felmlee, 1989), creating conditions to new developments (*i.e.* coronal *versus* axial, see Fig. 1 for details on image orientation). The improvement of the contrast achieved in the motion-corrected images by reducing the blurring motivated the research that is presented in this paper.

The objective of this work is assessing the capability of identifying seeds in mandarins using motion-corrected images. Features extracted by processing the motion corrected images are analysed with several statistical methods in order to establish the most reliable threshold for seed identification. Besides, the robustness

of the dynamic features was compared to the static values.

2. Material and methods

2.1. Samples

Mandarins cv Clemenules were obtained at a local market as potentially seedless fruits. Nardocott mandarins were provided by a citrus packinghouse in Valencia (Spain) and were expected to be seed-containing fruits as revealed in previous experiments. Samples were imaged at room temperature (22 °C).

A water-filled cube was used as test sample to correct the effect of the motion on the MR images.

2.2. Imaging equipment and fruit conveyor

The MRI experiments were performed on a Bruker BIOSPEC 47/40 (Ettlingen, Germany) spectrometer operating at 200 MHz (4.7 T). All experiments were performed with an actively shielded imaging gradient set provided with water refrigeration, which achieved 50 mT/m with corresponding rise time of 250 μ s. A radio frequency volume (birdcage) coil with an inner diameter of 20 cm was used.

Mandarins were conveyed through the coil at 54 mm/s rate by means of a specially designed conveyor belt (Hernández-Sánchez *et al.*, 2004).

2.3. Imaging sequences and motion correction within magnetic resonance images

In order to minimise motion artifacts, a fast imaging sequence was used. As revealed by a previous research (Hernández *et al.*, 2005) on seed detection in citrus, the fast low-angle shot sequence (FLASH) provides reliable results. The MR images were weighted by the effective

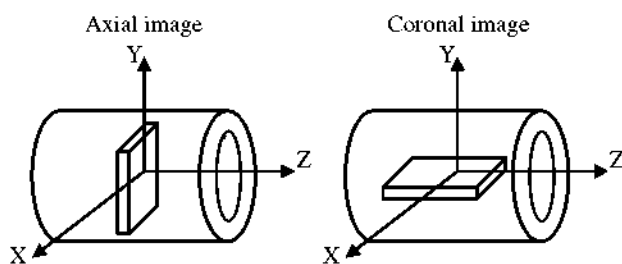


Fig. 1. Schematic of the magnet axis and the field-of-view orientation in axial magnetic resonance images, parallel to XY plane; and coronal MR images, parallel to XZ plane

transverse relaxation time T_2^* in order to maximise tissues differences. This imaging modality facilitates an optimal contrast between pulp and seed that leads to a better segmentation in the subsequent image analysis, still under reasonable time scale.

Coronal images (XZ plane) were obtained from mandarins placed with their central axis along the Y-axis of the magnet (see Fig. 1 for magnet axis). Such an orientation ensures that the tissue within the field-of-view (FOV) during the acquisition time remains unchanged. The phase encoding direction for MRI acquisition was selected along the X-axis, whereas the frequency encoding direction was selected along the Z-axis, which was indeed the motion direction.

The MRI sequence parameters were: recovery time (TR) of 11 ms, echo time (TE) of 3.8 ms and flip angle of 10° . The FOV and the slice thickness used were 12 cm by 12 cm and 12 mm, respectively. Images were collected with 64 by 128 acquisition matrix sizes and digitised with 4 byte unsigned integers. The total acquisition time was 703 ms. Pulse gains, attenuator, shimming settings as well as squared FOV location were adjusted for a mandarin with average dimensions (7 cm) located at the isocentre for static measurements whereas situated at 0 mm in the X direction, 10 mm in the Y direction and 0 mm in the Z direction from the isocentre for dynamic measurements. The shifted position from the isocentre in the Y direction is caused by the conveyor assembly itself. For both cases (dynamic and static), settings were held constant during the experiments. All images were zero-filled to 128 by 128 data before being reconstructed.

Image blurring due to phase shift during motion is corrected in the k -space (Fourier domain name of the reciprocal spatial space) prior to Fourier transformation of raw data. Such a correction procedure has been implemented and tested by Hernández *et al.* (2005) by means of several statistical features. In order to check the homogeneity of the conveyor speed, the displacement for each belt run is computed by acquiring navigator echoes of a cubic test sample.

One MR image was obtained from each mandarin at each run of the belt. Images were collected under stationary conditions (reference images) and during fruit conveying through the magnet at 54 mm/s belt speed. Three repetitions per fruit were performed in order to study the consistency of the subsequently extracted image features.

2.4. Reference measurements

After MRI, the mandarins were cut in halves through the equatorial section for inspection. Red green blue (RGB) images of the surfaces were captured with a digital camera for further analysis. Afterwards seeds

within the slice imaged by MR were both counted and weighted.

The RGB images were segmented by setting intensity thresholds so as to select those pixels belonging to the region of interest (ROI) and those pixels belonging to the central axis and seeds. The ratio between the areas of the hypo-intense region and the ROI for RGB images R_{sc} was computed for each fruit and compared to the corresponding values extracted from the MR images R_h by addressing the correlation coefficient.

2.5. Image processing and data analysis

2.5.1. Automated analysis

A number of features were automatically extracted from both the static and the motion-corrected dynamic images. Firstly, the ROI containing fruit tissues was selected within the image and the area A_{int} was computed in number of pixels. Then, the pixels with hypo-intense signals A_{hyp} in number of pixels are segmented within A_{int} . The value of A_{hyp} in number of pixels includes the tissue from the central axis as well as the seeds tissue. Once the value of A_{hyp} is identified, a number of features are extracted: (1) A_{hyp} to A_{int} ratio denoted by R_{st} ; (2) perimeter of A_{hyp} , P in number of pixels; (3) compactness of A_{hyp} , C computed as $4\pi A_{hyp} P^{-2}$ in pixel^{-1} ; (4) maximum distance from the centre of the A_{int} to the pixels belonging to P denoted by r_{max} in number of pixels; and (5) C to r_{max} ratio denoted by R_{cr} .

Features extraction was performed automatically since fruit sorting is required to be automated for on-line applications. Those features that allowed the best discrimination for mandarins with and without seeds were selected.

The algorithm applied for features extraction is an adaptation of that used by Hernández-Sánchez *et al.* (2004) in a work on detection of freeze injury in oranges.

2.5.2. Classification functions and validation

Several Nardocott mandarins revealed to be seedless fruits. Analysis of variance (ANOVA) was performed for comparison between the image features extracted from their respective MR images and those features extracted from the MR images of seedless mandarins variety Clemenule. As no significant differences were found between image features from fruits without seeds of different varieties those samples were grouped into a single cluster, which was regarded as the control set for further analysis.

In the second step, a new ANOVA was performed to address the image features presenting significant differences between the set of seedless fruits and that of fruits with seeds.

Significant features for classes discrimination were introduced into a forward stepwise discriminant analysis in order to obtain classification functions. Fisher value F for a variable to enter in the model was set to a high value of 3 so as to select only those variables with a high contribution to the discriminatory power of the model. Afterwards, the percentages of correct classification were calculated.

In order to reinforce the results from the classification function thresholds for seed identification were obtained from each feature as extracted from logistic regression at 50% probability.

Finally, the analysis was focused on validating the classification performance obtained by the discriminant analysis with static samples on mandarins imaged while conveyed through the spectrometer at 54 mm/s. Image features extracted from static and dynamic MR images were compared by means of an ANOVA in order to detect significant differences between acquisition conditions. The validation of the static model for sample classification was performed with the dynamic image features by addressing the percentage of correct classification. Metrology parameters and distance between the means of the fruit categories were analysed as potential sources of misclassification.

2.5.3. Metrology

Three MR images were obtained from each sample under both static and dynamic conditions for repeatability assessment. Image features were extracted from such MR images and the standard deviation (STD) over the three repetitions of each feature was computed. For each image feature STD was averaged over the 33 fruits imaged and the obtained value was used as an indicator of repeatability. The quality of the measurements was evaluated as the N/S ratio. The STD of an image feature over its three repetitions was taken as an estimator for the noise N (misaddressed variation), whereas the average value over those repetitions referred to the signal level S . Since comparison between features is dramatically affected by signal levels, measured range ($M_R = \text{maximum} - \text{minimum}$ value for all analysed sample units) has to be taken into consideration. Thus, the N/M_R ratio is computed as a more restrictive indicator than the N/S when addressing the quality of the statistical features. Both N/S and N/M_R were averaged over the 33 fruits.

3. Results and discussion

3.1. Seed identification under static conditions

According to visual inspection after cutting, 3 out of 15 Nardorcott mandarins had no seeds whereas only 1 out

of 18 Clemenules contained seeds. The characterisation of the fruits in terms of seeds and of the ratio R_{sc} extracted from the RGB images is presented in Table 1.

Figure 2 shows examples of MR images after motion correction of both seedless and seed containing mandarins. The ANOVA performed on the MRI features from seedless fruits (three repetitions per fruit) under static conditions revealed no significant differences between varieties for none of the MRI features: R_{sc} , P , C , r_{max} and R_{cr} (results not shown).

All the MRI features were significant for differentiating between seedless and seed-containing mandarins as stated by the ANOVA in Table 2. Significance levels were 1% except for compactness C with 5% significance

Table 1
Reference measurements [variety 1, Clemenules; variety 2, Nardorcott; number of seeds; and R_{sc} denotes the ratio of the seed and central axis region to the region of interest obtained from red green blue (RGB) segmentation]

Test no.	Variety	No. of seeds	Ratio (R_{sc}), %
<i>Mandarins without seeds</i>			
1	1	0	3.1
2	1	0	4.98
3	1	0	7.52
4	1	0	5.39
5	1	0	9.26
6	1	0	8.42
7	1	0	8.96
8	1	0	9.12
9	1	0	3.56
10	1	0	11.66
11	1	0	9.35
12	1	0	8.34
13	1	0	7.29
14	1	0	8.2
15	1	0	11.05
16	2	0	14.66
17	2	0	11.48
18	2	0	12.17
<i>Mandarins with seeds</i>			
19	1	1	9.79
20	2	1	11.28
21	2	1	11.88
22	2	1	14.29
23	2	1	13.93
24	2	1	12.01
25	2	1	15.74
26	2	2	12.52
27	2	3	12.31
28	2	3	18.12
29	2	3	12.69
30	2	4	20.75
31	2	4	13.3
32	2	5	13.66
33	2	5	15.28

level. Therefore the five features were introduced in the subsequent forward stepwise discriminant analysis using data from MRI stationary conditions. When using a

value for F of 3 to enter, only r_{max} was selected for the discriminant functions achieving a correct classification of 88.9% and 86.7% for seedless and seed-containing fruits, respectively.

Given the poor resolution of r_{max} (± 0.7 pixel) when compared to the distance between the means of seed and no seed categories (5 pixels, see Table 2), so that new discriminant analysis was performed excluding r_{max} . In this case the perimeter of the seed-axis region P was selected as unique variable. The new discriminant functions allowed an 81.5% and 86.7% classification for seedless and seed-containing fruits, respectively, indicating a reduction in the classification performance. Since the resolution for P (± 1 pixel) is high with regard to the distance between seed and no seed categories, (25 pixels, see Table 2), it was decided to generate classification functions including both parameters, r_{max} and P , taking advantage of their valuable individual characteristics. The percentages of mandarins correctly classified using r_{max} and P were the same as those for r_{max} discrimination. Figure 3 shows the relative position of the fruits with respect to the threshold line computed as the intersection between the discriminant functions. Samples above the line are classified as seed-containing fruits and samples below line as seedless fruits.

A metrology study on the MRI stationary features shows that P and r_{max} are the parameters with the lowest N/S ratio, consequently, being the most robust (Table 3). Their N/S values are about 4% whereas those of the others features are bounded to 14%. The values computed for samples under motion conditions are very similar to those obtained from the stationary samples highlighting the high effectiveness of the motion correction procedure. When the noise is compared to

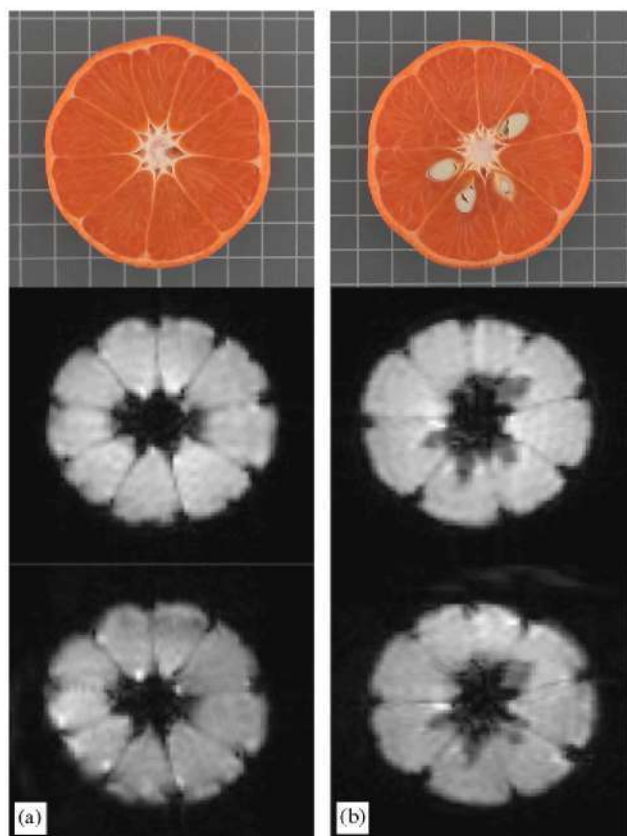


Fig. 2. Examples of (a) seedless and (b) seed-containing mandarins; upper line corresponds to red green blue (RGB) images; middle line to static magnetic resonance images, and bottom line to motion-corrected magnetic resonance images

Table 2
Analysis of variance on seed influence for the features extracted from the static and dynamic motion-corrected magnetic resonance images (*, significance at 5%; ** significance at 1%).

Parameter	Without seeds ($n = 18$)	With seeds ($n = 15$)	Fisher value (F)	Probability (p)
<i>Static MR images</i>				
Ratio R_h	12.1 ± 3.3	16.5 ± 3.2	14.81	**
Perimeter P , pixel	73.1 ± 14.4	97.9 ± 14.8	23.82	**
Compactness C , pixel^{-1}	0.7 ± 0.1	0.6 ± 0.1	4.73	*
Radius r_{max} , pixel	12.7 ± 2.2	17.7 ± 2.3	38.23	**
Ratio R_{cr}	5.73 ± 1.86	3.32 ± 0.93	17.63	**
<i>Dynamic MR images</i>				
Ratio R_h	11.3 ± 3.7	15.4 ± 2.9	11.18	**
Perimeter P , pixel	70.8 ± 12.3	97.7 ± 14.1	34.38	**
Compactness C , pixel^{-1}	0.7 ± 0.1	0.6 ± 0.1	9.19	**
Radius r_{max} , pixel	12.7 ± 2.4	16.9 ± 1.9	31.71	**
Ratio R_{cr}	5.50 ± 1.37	3.36 ± 0.80	28.60	**

N , number of observations; R_h , hypo-intense signal region to region of interest ratio; R_{cr} , compactness to radius ratio.

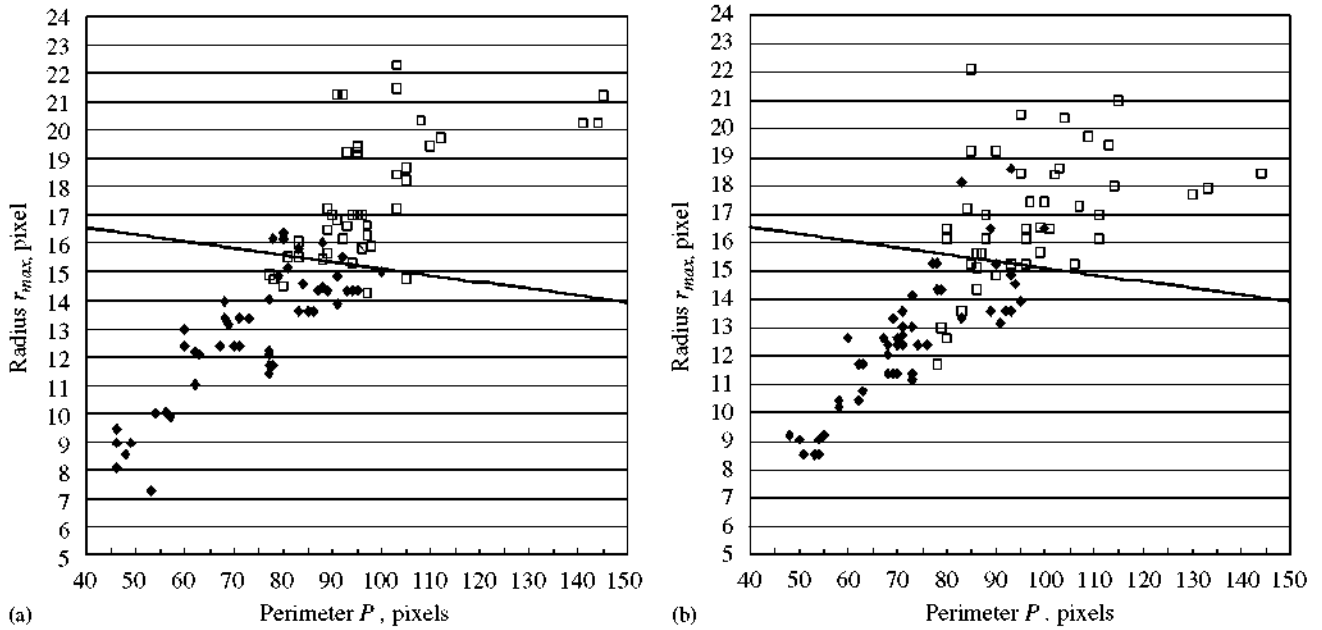


Fig. 3. Computed values for the perimeter of the seed-axis area (P) and the maximum radius (r_{max}) for mandarins without and with seeds (3 replicates per fruit): (a) static measurements; and (b) dynamic measurements; \blacklozenge , without seeds; \square , with seeds; detection threshold of discriminant functions

Table 3
Metrological features for magnetic resonance images under static and dynamic conditions

Parameter	Noise to signal ratio (N/S), %		Noise to measured range ratio (N/M_R), %	
	Static	Dynamic	Static	Dynamic
Ratio R_h	9.29	7.3	6.84	6.77
Perimeter P	3.87	4.9	3.18	4.98
Compactness C	11.28	7.57	15.5	9.81
Radius r_{max}	4.14	5.81	4.3	8.13
Ratio R_{cr}	13.65	10.81	7.45	6.9

R_h , hypo-intense signal region to region of interest ratio; R_{cr} , compactness to radius ratio.

the range instead of the average signal, P and r_{max} have the lowest values of all the MRI parameters. Such results also point out to their high discriminant capability since low error levels compared to maximum differences between fruits are found. Nevertheless, the N/M_R values of the rest of MRI features are also acceptably low (below 16%).

Logistic regressions were performed with the whole set of MRI data (99 images) that included the three repetitions for each fruit. The feature that showed the best fit on the basis of a minimum overlapping between categories was the perimeter of seed-axis area P . The threshold value at 50% probability between seedless and

seed-containing classes was 87.5 pixels confirming the previous result. The threshold value can also be extracted from r_{max} and R_{cr} although segregation is not as satisfactory.

In order to enhance identification of mandarins with seeds, as demanded by the worldwide trade, experimental conditions will be improved in future studies. A larger sample of fruits of the same variety will lead to more reliable results in the development of classification functions by means of statistical analysis. Besides, setting uncertainty bands for the classification thresholds would become feasible allowing the optimization of misclassification errors.

3.2. Seed identification under dynamic conditions

The acquisition of coronal images has involved a noticeable improvement in the quality of the image acquired under dynamic conditions since the motion correction procedure achieves a high level of blurring suppression and consequent enhancement of tissue contrast. A simple visual inspection of the dynamic MR images shows that the contrast between tissues and the definition of their edges are rather comparable to those of the static images. Therefore, the blurring in axial images, showed as the main hindrance for image processing (Hernández-Sánchez *et al.*, 2004), is overcome when coronal images are obtained and motion correction is performed. Moreover, the algorithms developed to be applied for the stationary samples can be easily transferred to dynamic conditions, which is very convenient for the development of new applications on the basis of previous knowledge.

The improvement in the quality of coronal (motion corrected) images with respect to that of the axial dynamic images is highlighted not only by the metrological features (N/S , N/M_R) but also by the correspondence between the features extracted from the RGB and the MR images: R_{sc} and R_h respectively (Fig. 4). The correlation coefficient between both parameters is 0.8 for static MRI and 0.7 for dynamic MRI.

Dynamic MRI features are not significantly different from those obtained under static conditions but are significantly different between seedless and seed-containing mandarins (5% significance levels), reinforcing the similarities between static and dynamic features (Table 2).

In order to validate the classification performance obtained by the discriminant analysis with static samples, images on mandarins conveyed through the spectrometer at 54 mm/s were automatically corrected for motion blurring (Fig. 2) and MRI features were subsequently extracted and used within previous classification functions. The proportions of correct classification were 92.5% and 79.5% for the seedless and seed-containing category, respectively.

A higher number of mandarins without seeds were correctly sorted under motion conditions (from 88.9% under static to 92.5% under dynamic conditions) when compared to static inspection. In contrast, the classification performance decreases for fruits with seeds (from 86.7% to 79.5% under static and dynamic conditions respectively). In this work, it was feasible to detect single seed fruit which was undetectable with axial images without motion correction (Hernández-Sánchez *et al.*, 2004). The fact that the lowest percentage of correct classification occurs for seed containing fruits is counter to the main interest of the market.

The decrease in classification performance was initially ascribed to the dispersion in the values of r_{max}

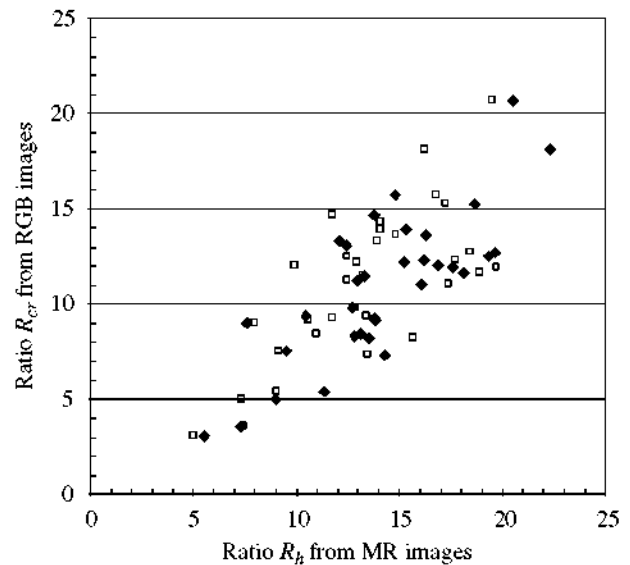


Fig. 4. Comparison of red green blue (RGB) and magnetic resonance (MR) images according to the ratio between the region including seeds and central axis with regard to the region of interest; the results for MR image segmentation (R_h) and RGB image segmentation (R_{sc}) are shown per fruit (no. of observations, $n = 33$; \blacklozenge , static; \square , dynamic).

for dynamic measurements, involving a decrease in the values of some of the repetitions corresponding to samples with seeds, which are wrongly classified as seedless fruits (Fig. 4). Thus, for each of the MRI features of interest it was decided to evaluate changes in categories distance. Results indicated that the distance under motion conditions increases slightly for P and clearly for C , whereas the other features show high approximation between seedless and seed-containing category, that is losing discrimination ability. For r_{max} distance under dynamic conditions is reduced about a 13% of the value obtained from stationary samples (Table 4), which involves increasing difficulties for fruit discrimination. Nevertheless, the ANOVA for static and dynamic MRI features showed no significant differences between acquisition conditions (see Table 2 for average static and dynamic values).

The metrological study showed that the errors under motion conditions are slightly higher than those computed under static conditions for r_{max} and P (see Table 4) pointing to a possible cause for misclassification. Nevertheless, the overall incidence of the noise remains below 6% for such dynamic MRI features, which reinforces their use for the discrimination of the fruits. The low differences in N/S and N/M_R ratios between static and dynamic features highlight the robustness of the motion correction procedure.

Table 4

Variation of the distance between seedless and seed-containing category expressed as a proportion (in percentage) of the static value when magnetic measure images are obtained under dynamic conditions for each magnetic resonance imaging (MRI) parameter

Parameter	Variation in categories distance (%)
Ratio R_h	-19.84
Perimeter P	0.97
Compactness C	15.15
Radius r_{max}	-13.33
Rates R_{cr}	-12.52

R_h , hypo-intense signal region to region of interest ratio; R_{cr} compactness to radius ratio.

4. Conclusions

The features extracted from motion-corrected images are statistically indistinguishable from those of the static ones as determined by the analysis of variance (ANOVA) and metrological parameters noise-to-signal ratio and noise-to-measured range ratio (N/S , N/M_R). The maximum radius and the perimeter of the seeds-axis area have been addressed as the most relevant features for identifying seed-containing mandarins.

A main conclusion of this study is that it is feasible to perform a straightforward export of models developed under static conditions towards on-line conditions.

Acknowledgements

We thank the Spanish Science and Technology Ministry for financing and DAUMAR S.A. for designing and building the conveyor.

References

- Barreiro P; Ruiz-Altisent M; Valero C; García-Ramos F J** (2004). Fruit postharvest technology: instrumental measurement of ripeness and quality. In: *Quality Handling and Evaluation*, pp 321–340. Kluwer Academic Publishers, Netherlands
- Blasco J; Alamar M C; Moltó E** (2003). Detección no destructiva de semillas en mandarinas mediante Resonancia Magnética [Non destructive detection of seeds in mandarins by using Magnetic Resonance.] *Resúmenes del II Congreso Nacional de Agroingeniería*, Córdoba, Spain, pp 439–440
- Ehman R L; Felmlee J P** (1989). Adaptive technique for high-definition MR Imaging of moving structures. *Radiology*, **173**, 255–263
- Hernández-Sánchez N; Barreiro P; Ruiz-Altisent M; Ruiz-Cabello J; Fernández-Valle M E** (2004). Detection of freeze injury in oranges by magnetic resonance imaging of moving samples. *Applied Magnetic Resonance*, **26**, 431–445
- Hernández N; Barreiro P; Ruiz-Altisent M; Ruiz-Cabello J; Fernández-Valle M E** (2005). Detection of sedes in citrus using MRI under motion conditions and improvement with motion correction. *Concepts in Magnetic Resonance B*, **26B**, 81–92
- Hills B P; Clark C J** (2003). Quality assessment of horticultural products by NMR. *Annual Reports on NMR Spectroscopy*, **50**, 75–120